Journal of Fluids and Structures 17 (2003) 903–913

JOURNAL OF FLUIDS AND STRUCTURES

www.elsevier.nl/locate/jnlabr/yjfls

Flow control around a circular cylinder by internal acoustic excitation

N. Fujisawa*, G. Takeda

Department of Mechanical and Production Engineering, Niigata University, 8050 Ikarashi 2, Niigata 950-2181, Japan

Received 20 November 2001; accepted 10 March 2003

Abstract

The possible drag reduction and the corresponding variation of the flow field around a circular cylinder are studied in a wind tunnel using flow control with acoustic excitation, which is supplied internally through a slit to the flow over the cylinder. The drag and the lift force acting on the cylinder are evaluated from the measurement of pressure distributions over the cylinder. The results indicate that the drag is reduced about 30% in comparison with a stationary cylinder, when the control parameters are optimized, such as the slit angle, the forcing Strouhal number and the excitation amplitude. The corresponding flow field around the cylinder with and without control is measured by particle image velocimetry. It is found that the wake of the circular cylinder is elongated downstream and the streamwise mean velocity is accelerated on both sides of the cylinder by the influence of acoustic excitation. On the contrary, the velocity fluctuations and the Reynolds stress in the near wake of the cylinder are strongly diminished under acoustic excitation. These variations of the wake flow support the drag reduction observed in the present measurements.

1. Introduction

The drag reduction and the flow management over a circular cylinder are important research topics related to the engineering problems of flow-induced vibration and noise of bluff-body structures. Therefore, the fluid forces acting on the circular cylinder in a flow stream and the mechanisms of vortex formation behind it have been investigated in the literature, which are summarized in some review papers by Sarpkaya (1979), Bearman (1984), Griffin and Hall(1991) and others. Nowadays, the passive techniques called vortex suppression devices have been studied and they are applied to a bluff-body structure in a stream to avoid vortex-induced vibrations on engineering problems. These devices disrupt or prevent the formation of organized two-dimensional structures of vortex shedding. This topic is reviewed by Blevins (1990). On the other hand, the active techniques for controlling the vortex shedding from a circular cylinder have been investigated more recently, but the studies are rather limited in comparison to those with passive techniques. Some investigators introduced acoustic disturbances (Blevins, 1985; Hsiao and Shyu, 1991) and velocity disturbances (Tokumaru and Dimotakis, 1991; Filler et al., 1991; Fujisawa et al., 1998) into the wake of a circular cylinder to understand the influence on vortex shedding. It is found that vortex shedding can be attenuated under certain conditions of the imposed disturbances (Hsiao and Shyu, 1991; Tokumaru and Dimotakis, 1991), but the mechanism of flow control is not well understood. These active techniques have been further studied by introducing a feedback control to the flow around the cylinder to promote the control effect, as investigated by Ffowcs Williams and Zhao (1989), Roussopoulos, (1993), Huang (1996), Warui and Fujisawa (1996), Fujisawa et al. (2001) and others. These approaches are very attractive in application to engineering problems of flow control, where the introduction of the

*Corresponding author. Tel., fax: +81-25-262-6726.
E-mail address: fujisawa@eng.niigata-u.ac.jp (N. Fujisawa).

0889-9746/03/$ - see front matter
doi:10.1016/S0889-9746(03)00043-4

passive technique is difficult to apply for various reasons. Among the variety of such active control techniques, the internal acoustic excitation technique is one very suitable for controlling the external flow around a bluff-body structure in a flow-stream, because the actuator device can be installed inside the structure without any geometrical modification.

Hsiao and Shyu (1991) investigated the effect of acoustic excitation introduced internally to a circular cylinder through a slit to improve the aerodynamic performance of the cylinder in a uniform flow. They emitted the acoustic disturbances from a speaker system through the slit to the flow over the cylinder with sound pressure levels as high as 130 dB. The dimension of the slit was 1 mm wide and 80 mm long, while the cylinder diameter was 60 mm with the length 200 mm, so that the aspect ratio of the cylinder was as small as 3.3. The drag was evaluated from wake velocity measurements and was found to be reduced by up to 40% at the optimum condition of the forcing frequency and slit location at a Reynolds number 2×10^4. However, the measurement of pressure distributions did not indicate any drag reduction, which suggests that further research should be conducted to confirm the drag reduction by the acoustic excitation.

The purpose of the present paper is to investigate the possible drag reduction and the corresponding variations of the flow field around a circular cylinder under acoustic excitation introduced through a slit located over the whole span of a cylinder. Based on these results, the aerodynamic performance under the influence of acoustic excitation and the mechanism of drag reduction of the circular cylinder are studied in detail.

2. Experimental apparatus and procedures

2.1. Flow control by acoustic excitation

A schematic illustration of flow control technique is given in Fig. 1. A circular cylinder having a diameter d is located in a uniform flow-velocity U_0. The acoustic excitation is provided inside the cylinder and supplied to the flow over the cylinder through a slit, where the angle of the slit against the free-stream velocity is β. The flow field around the circular cylinder under such acoustic control can be described by the nondimensional parameters, such as forcing Strouhal number $S_f(=fd/U_0)$, velocity amplitude $V_r(=v/U_0)$ and Reynolds number $\mathrm{Re}(=U_0d/\nu)$, where f is the frequency of acoustic excitation, v is the maximum flow velocity through the slit, and ν is the kinematic viscosity of fluid.

2.2. Experimental apparatus and pressure measurement

The present experiment was carried out using an open-jet type wind tunnel. The schematic diagram of the experimental test section is shown in Fig. 2. The test cylinder has an outer diameter $d = 50$ mm and an inner diameter 40 mm, which is located at 200 mm downstream of the contraction nozzle of the open-jet wind tunnel, which has a cross-sectional area of 500 mm×500 mm. The nonuniformity of the free-stream velocity was found to be 1%, and the streamwise turbulence intensity was 0.8% in the central cross-sectional area of 400 mm×400 mm. The test cylinder was supported by two vertical sidewalls of the test-section, which are made of transparent material for flow visualization purposes. In order to maintain the two dimensionality of the flow field, the end plates having an area of 430 mm×400 mm are attached on both ends of the cylinder at a distance of 50 mm from the vertical sidewalls to remove the oncoming boundary layers (Szeppesy and Bearman, 1992). Therefore, the aspect ratio of the test cylinder was kept to 8 in the present experiment. The top and bottom boundary of the test-section were made free. It is to be noted that the natural Strouhal frequency of vortex shedding is found to be $S_{f0}(=f_0d/U_0) = 0.23$ in the present stationary cylinder without a slit, where f_0 is a natural frequency of vortex shedding.

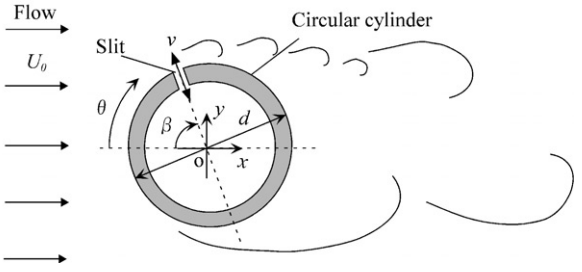

Fig. 1. Schematic illustration of flow geometry.

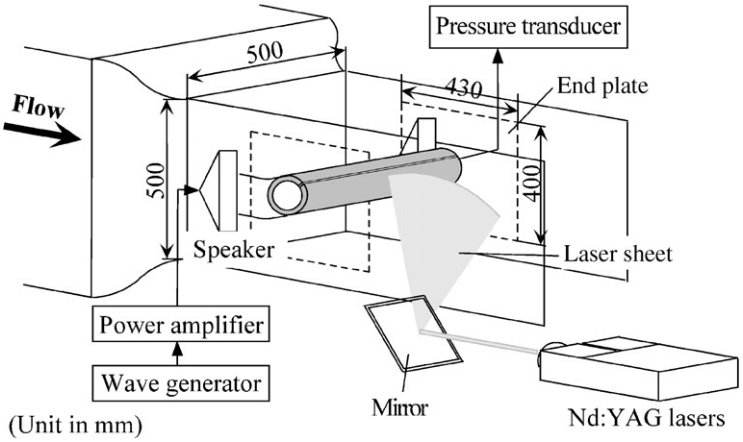

Fig. 2. Experimental arrangement for flow control in wind tunnel.

The circular cylinder had a spanwise slit-structure having uniform width of 0.4 mm with full span of 400 mm. The angle of the slit, β could be set to an arbitrary value by rotating the cylinder. The acoustic sounds were emitted from two loud speakers of maximum input power of 300 W, which were located at both ends of the cylinder. The loud speaker was driven by a sinusoidal wave-generator in combination with a power amplifier. The r.m.s. value of the pressure fluctuation inside the circular cylinder was found to be uniform over the central spanwise distance of 300 mm with an accuracy of $\pm 3\%$ in the frequency range ($f = 12$–60 Hz) for the present experiment. In order to evaluate the velocity amplitude V_r of the acoustic excitation, the maximum velocity v at the exit of the slit was measured by a single probe hot-wire anemometer.

The pressure distribution over the circular cylinder was measured by a pressure transducer of straingauge type (maximum pressure 50 Pa), which is fixed at one end of the cylinder. Thirty-five pressure holes of 0.6 mm in diameter were distributed over the mid-plane of the cylinder at every 10° in circumferential direction, except for the slit location. The pressure hole and the pressure transducer were connected by a stainless-steel tube 0.9 mm in inner diameter. The drag and lift forces were evaluated by integrating the pressure distribution over the cylinder surface. The experiment was carried out at a free-stream velocity of 2.6 m/s, which corresponds to Reynolds number $\mathrm{Re} = 9 \times 10^3$.

2.3. Flow-field measurement by PIV

The flow field around a circular cylinder under acoustic excitation was measured by particle image velocimetry. A schematic illustration of the PIV measurement is shown in Fig. 2. The tracer particles of smoke were generated from the smoke machine located at the inlet of the wind tunnel blower. In order to observe the flow field around the circular cylinder, the flow field was illuminated by a light sheet from a pair of Nd:YAG pulse lasers, which emit 532 nm wavelength light at a pulse width 5 ns with a pulse rate 15 Hz for each laser. The pulse energy of these lasers is 50 mJ per pulse, which is strong enough to observe the smoke particles in an area of 100 mm × 100 mm by the monochrome digital CCD camera having a spatial resolution of 1008×1018 pixels with 8 bits in gray level. The camera was operated in a double exposure mode and was synchronized with the pulse signal from a pulse generator installed to a personal computer, which also controlled the instant of the laser illumination. The time interval between the successive laser-pulses was set to 80 μs in the present measurement. The captured digital images were stored on a frame memory of the personal computer. The target image in the present experiment had an actual size of 100 mm × 100 mm, so that the spatial resolution of the captured image is about 0.1 mm/pixel. However, the whole flow-field around the cylinder, 150 mm × 250 mm, was measured in the present study by traversing the CCD camera. The instantaneous velocity distributions were analyzed by using a gray-level difference algorithm for the cross-correlation calculation between two successive images. The sizes of the interrogation window and search window were set to 30×30 pixels and 44×44 pixels, respectively, which combination was found to minimize the error vectors with enough spatial resolution. The sub-pixel interpolation process was incorporated into the analysis to improve the accuracy of the velocity measurement. The statistical properties of the flow field were evaluated from 300 instantaneous velocity distributions in the present experiment. The uncertainty interval of velocity measurement at 95% coverage was found to be 3% in the present experiment.

3. Results and discussions

3.1. Pressure distributions over a circular cylinder

The pressure distributions over the circular cylinder were measured to study the influence of acoustic excitation through the slit. Fig. 3 shows the measured pressure distributions over a circular cylinder at various combinations of the slit angle β and the forcing Strouhal numbers S_f, where the pressure coefficient is defined by $C_p(=2(p-p_f)/\rho U^2)$. Here, p is the static pressure over the circular cylinder and p_f is the free-stream pressure. It is to be noted that the velocity amplitude V_r is set to an optimum value 1.5 in this figure. The influence of V_r on the drag and lift force will be studied in the next section.

Fig. 3(a) shows the pressure distributions over a circular cylinder with acoustic excitation at the natural frequency of vortex shedding, that is $S_f = S_{f0}$. The result indicates a small influence of acoustic excitation on the pressure distributions, which appears at the slit angles $\beta = 75$–90° and over the cylinder near the slit location. The pressure behind the cylinder is decreased by the influence of acoustic excitation in comparison with the case without control, which appears strong especially at $\beta = 90^\circ$. When the forcing Strouhal number S_f increases to $2S_{f0}$ (Fig. 3(b)), the influence of acoustic excitation on the pressure distribution becomes more dominant and the decreased pressure region appears over a wider range of the cylinder surface than for the case of $S_f = S_{f0}$. On the other hand, the behavior of the pressure distribution changes quickly, when the acoustic excitation is given at $S_f = 4S_{f0}$ (Fig. 3(c)), which corresponds to the unstable frequency of the separating shear-layer. In most of the slit angles except for $\beta = 90^\circ$, the pressure distribution over the circular cylinder indicates a pressure decrease near the slit location, which is similar to the

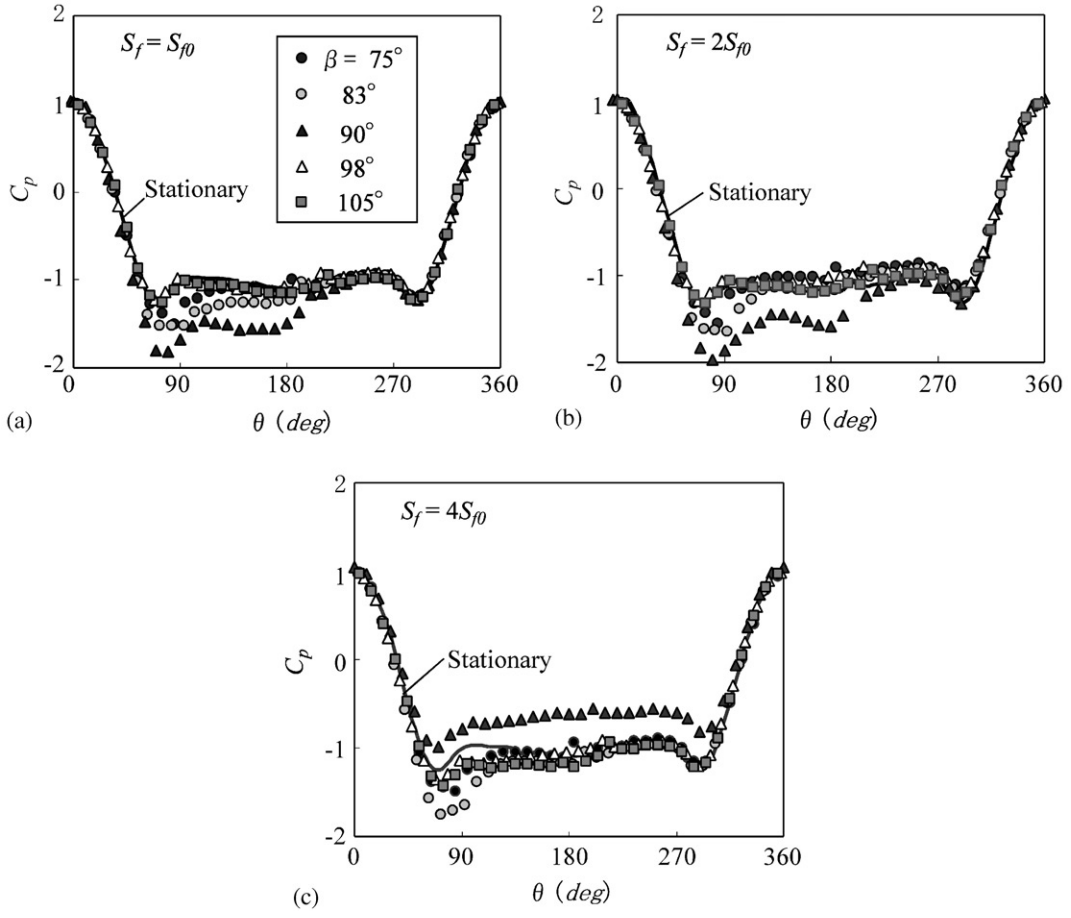

Fig. 3. Pressure distributions over a circular cylinder at various slit angles under acoustic excitation ($V_r = 1.5$): (a) $S_f = S_{f0}$; (b) $S_f = 2S_{f0}$; and (c) $S_f = 4S_{f0}$.

influence of acoustic excitation observed at smaller forcing frequencies. However, the pressure behind the cylinder at $\beta = 90^\circ$ shows an abrupt increase over the whole area behind it. This is a direct evidence of drag reduction of the circular cylinder by acoustic excitation, although this was not observed in the experiment by Hsiao and Shyu (1991). The present results indicate that the most effective slit angles are around $\beta = 90^\circ$, which agrees roughly with the experiment by Hsiao and Shyu (1991), who found the optimum slit angle $\beta = 80^\circ$ from wake velocity measurements. It can be seen from the present pressure distribution measurements that the separation point, which corresponds to the point of minimum pressure, is not influenced by the acoustic excitation and stays around 80°. Therefore, the most effective slit angle is considered to be just downstream of the separation point. It is expected that the separating shear-layer is synchronized to the unstable frequency of acoustic excitation and that the velocity distribution along the shear layer is modified so as to increase the pressure behind the separation point.

3.2. Fluid force characteristics

Fig. 4 shows the drag and lift force characteristics of the circular cylinder under the acoustic excitation, which is evaluated from the measurement of pressure distributions. The drag and lift force coefficients are defined by $C_d(= 2F_x/\rho U^2)$ and $C_l(= 2F_y/\rho U^2)$, respectively, where F_x and F_y are streamwise and normal fluid forces acting on the cylinder, respectively. These characteristics are plotted against the slit angle β in Fig. 4(a), the forcing Strouhal number S_f in Fig. 4(b) and the velocity amplitude V_r in Fig. 4(c) to determine the optimum control parameters.

It is evident from Fig. 4(a) that the drag coefficient C_d can be minimized by the acoustic excitation, when it is emitted around the slit angle $\beta = 90^\circ$ and excited at the unstable frequency of the shear layer $4S_{f0}$ with a velocity amplitude $V_r = 1.5$. This result indicates that the synchronization of the shear layer by the acoustic excitation is limited to a small range of slit angles and that the acoustic excitation just behind the separation point effectively enhances the growth of the instability in the shear layers. On the other hand, a positive lift force is generated on the cylinder for β around 83° by the acoustic excitation at $S_f = 4S_{f0}$. This is due to the formation of asymmetrical pressure distributions over the cylinder surface by the presence of the one-side slit.

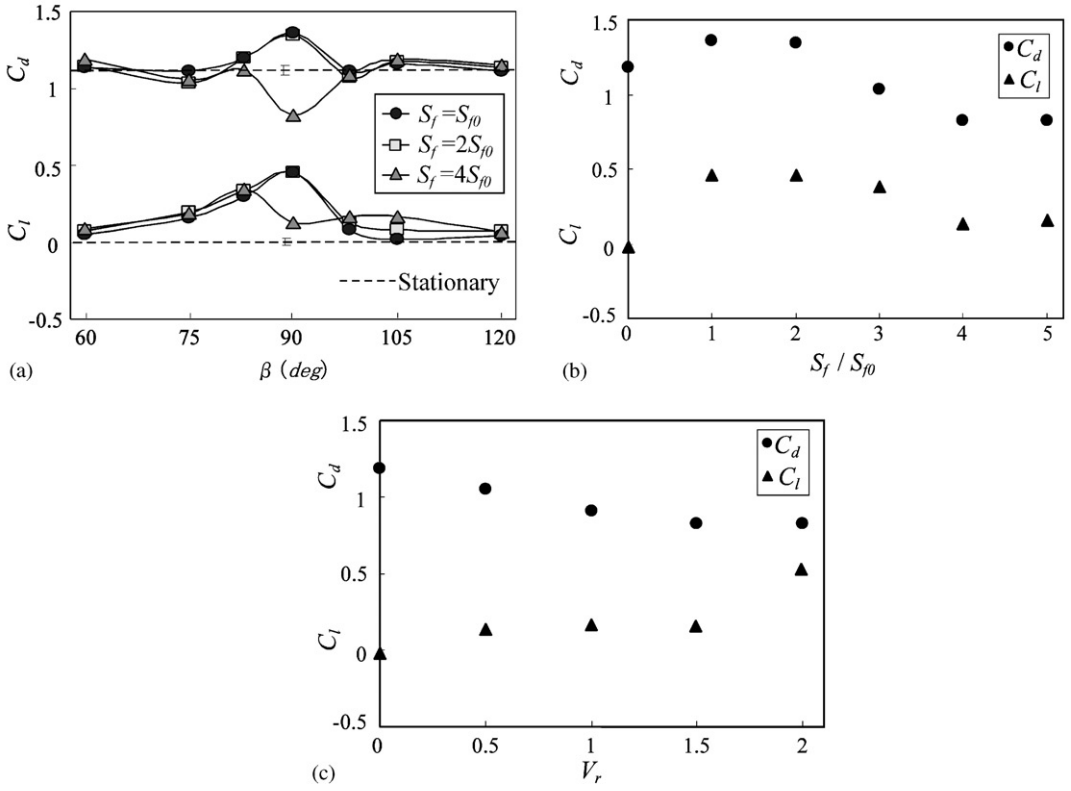

Fig. 4. Variations of drag and lift coefficient with respect to control parameters: (a) slit angle ($V_r = 1.5$); (b) forcing Strouhal number ($\beta = 90^\circ$, $V_r = 1.5$); and (c) velocity amplitude ($\beta = 90^\circ$, $S_f = 4S_{f0}$).

The influence of the forcing Strouhal number on the drag and lift coefficients is shown in Fig. 4(b), where $\beta = 90^\circ$ and $V_r = 1.5$. With an increase in forcing Strouhal number S_f, the drag coefficient C_d increases to a maximum around $S_f = 2S_{f0}$ and then it decreases to a smallest value around $S_f = 4S_{f0}$. This result suggests that the most effective forcing frequency corresponds to the unstable frequency of the shear layer. The variation of the lift coefficient C_l with S_f is very similar to that of C_d, which also reflects the asymmetrical pressure distribution around the cylinder due to the slit location. It is considered that the increase in C_d around $S_f = S_{f0}$ and $2S_{f0}$ is expected to be due to the synchronization of the vortex shedding from the circular cylinder with the acoustic excitation, while the drag reduction observed at $S_f = 4S_{f0}$ is expected to be caused by the synchronization of the separating shear-layer from the slit side of the circular cylinder.

Fig. 4(c) shows the influence of the velocity amplitude V_r on the drag and lift coefficients on the circular cylinder, where $\beta = 90^\circ$ and $S_f = 4S_{f0}$. With an increase in V_r, the drag decreases gradually, and this trend becomes saturated at V_r larger than 1.5. On the other hand, the lift force increases gradually with V_r and it grows suddenly at V_r larger than 2. This sudden increase in C_l is found to be caused by the appearance of a low-pressure region near the slit location. Therefore, it is expected that a further increase in V_r may create a larger lift force without improving the drag.

These discussions will lead to the following conclusion about the optimum combinations of the control parameters of acoustic excitation. The drag of a circular cylinder can be controlled optimally by forcing the separating shear-layer just downstream of the separation point with the forcing frequency around the unstable frequency of the shear layer $S_f = 4S_{f0}$, and at the velocity amplitude around $V_r = 1.5$. The maximum drag reduction of 30% was observed at the optimum condition of acoustic excitation and at Reynolds number $\mathrm{Re} = 9000$.

3.3. Flow field around a circular cylinder

In order to understand the mechanism of drag reduction of circular cylinder by the optimum acoustic excitation, the flow field around the circular cylinder was measured by particle image velocimetry. Fig. 5 shows the velocity vectors and the contour of velocity magnitude around the circular cylinder under the acoustic excitation (Fig. 5(a)), which is compared with that of the stationary cylinder (Fig. 5(b)). The control parameters in the acoustic excitation are set to the optimum condition for drag reduction, such that the slit angle is $\beta = 90^\circ$, the forcing Strouhal number $S_f = 4S_{f0}$ and the velocity amplitude $V_r = 1.5$. It is clearly seen that the wake region of the circular cylinder is fairly elongated downstream by the influence of the optimum acoustic control. The contour of the high-velocity area on both sides of the cylinder is extended to the downstream, which indicates the acceleration of the side flow by the influence of the velocity deficit in the wake of the cylinder. Corresponding to the variations of the wake velocity distribution, the width of the cylinder wake is reduced by the optimum acoustic control, which can be seen in the contour of the velocity magnitude in the wake ranging from $x/d = 1.5$ to 4.

Figs. 6(a) and (b) shows the contour of velocity fluctuation in the wake of the circular cylinder with and without acoustic control, respectively. It is to be noted that the velocity fluctuation shown here is defined by the total velocity fluctuation $\sqrt{u'^2 + v'^2}$, which is composed of the periodic velocity and turbulence fluctuation. The magnitude of the

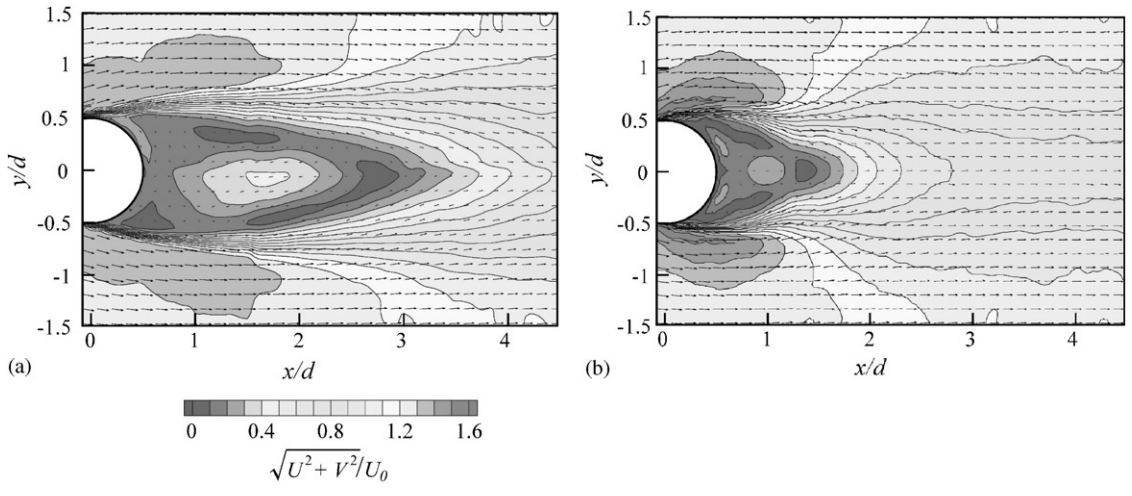

Fig. 5. Velocity vectors and contours of velocity magnitudes: (a) optimum acoustic control and (b) without control.

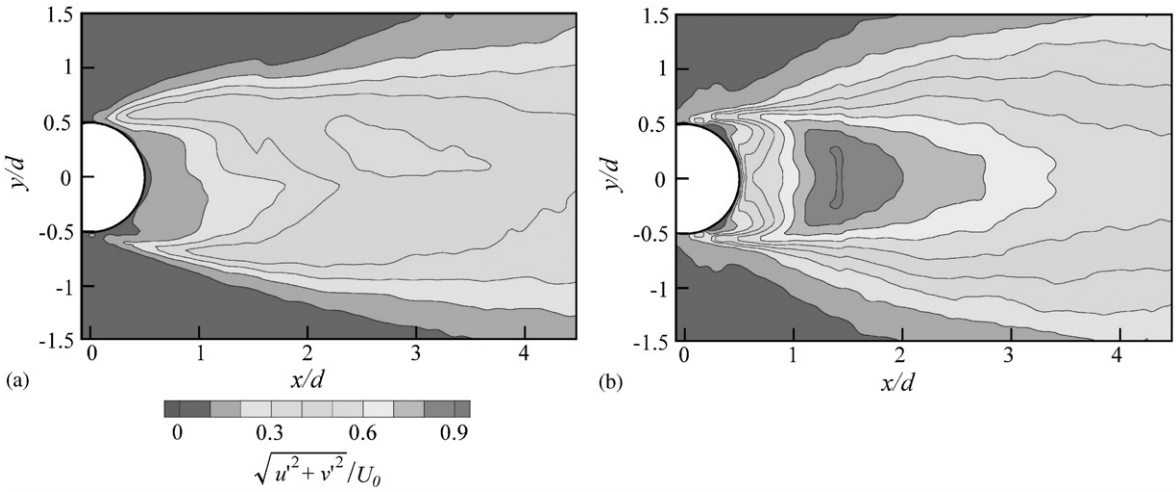

Fig. 6. Contours of velocity fluctuation: (a) optimum acoustic control and (b) without control.

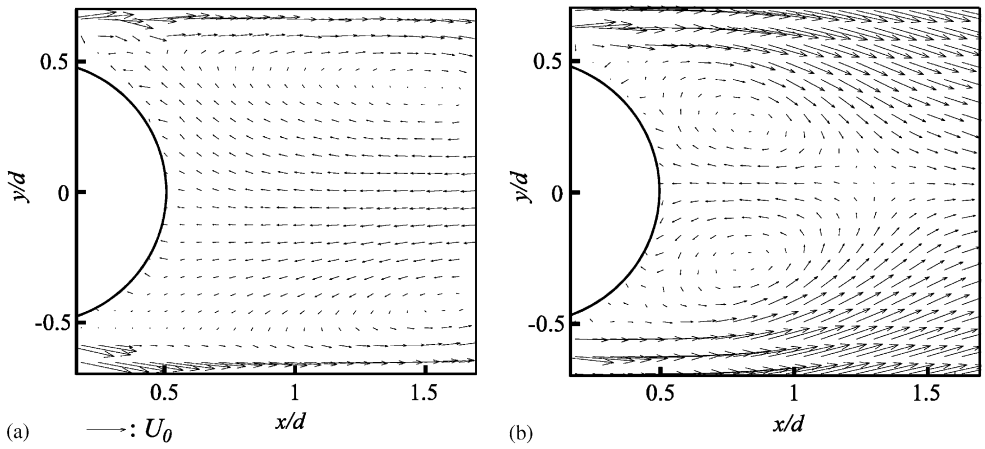

Fig. 7. Close-up view of velocity vectors in near-wake region: (a) optimum acoustic control and (b) without control.

velocity fluctuation is suppressed strongly by the optimum acoustic control in the near-wake region of the cylinder, which ranges from $x/d = 0.5$ to 3. The reduction in the wake width by the influence of the control is also observed in this contour map, which is very similar to the result of velocity magnitude in Fig. 5. These results indicate that the drag of the circular cylinder can be reduced by the modification of the mean-velocity distribution and the corresponding reduction of the velocity fluctuations in the wake of the circular cylinder by the influence of acoustic excitation.

3.4. Near-wake velocity field

Fig. 7(a) shows the close-up view of mean-velocity vectors in the near-wake region under the optimum acoustic control, which is compared with the case without control in Fig. 7(b). The flow around the circular cylinder without control (Fig. 7(b)) indicates the presence of two regions of recirculating flow in the near-wake of the cylinder. Therefore, the side flows over the cylinder go over the recirculating region behind the cylinder and approach closer to each other downstream of this region. On the other hand, the mean-velocity distribution near the cylinder is modified by acoustic control strongly, as shown in Fig. 7(a). The recirculating region near the cylinder is removed and the small area of recirculating region is produced near the separating shear-layer downstream of the cylinder. Hence, a mean reverse flow is created over a wide area behind the cylinder by the optimum acoustic control, which indicates a rather uniform

velocity distribution in the wake of the cylinder and results in the generation of smaller turbulent kinetic energy behind the cylinder than in the case without control.

3.5. Cross-sectional distributions of statistical flow properties

The cross-sectional distributions of the mean velocity U and V, the velocity fluctuation u' and v' and the Reynolds stress $\overline{uv}$ in the wake of the circular cylinder are displayed in Fig. 8 at four positions $x/d = 1$, 2, 3 and 4 in the cylinder wake, where the result under optimum acoustic control is compared with the stationary cylinder. The mean-velocity distributions under optimum acoustic control indicate the development of a wake flow behind the cylinder ($x/d = 1$), which can be seen by the increase in the wake velocity deficit in U and the appearance of outward spreading in V. It is noted that the large inward velocity V appears in the stationary cylinder at the same position x/d, which is due to the presence of the recirculating region behind the cylinder. When the streamwise distance increases to $x/d = 2$, the wake velocity deficit remains large in U, but the inward velocity is created in V similar to the case without control. Corresponding to the large velocity deficit in the cylinder wake caused by the optimum acoustic control, the mean velocity U on both sides of the cylinder still remains at a large value, which contributes to the drag reduction observed in the pressure measurement. On the other hand, the mean velocity U on the cylinder side without control is decreased by the spreading effect of the cylinder wake normal to the free stream. In the downstream $x/d = 3$ and 4, the mean-velocity distributions U, V under the control are in a relaxation process and they tend gradually to that of the case without control; however, the deviation can still be observed even in the velocity profiles at $x/d = 4$. It is to be noted that the negative velocity in U disappears in the downstream for $x/d > 2.8$ under optimum acoustic control, while $x/d > 1.4$ for the case without control. This result indicates the elongation of the cylinder wake by the optimum acoustic control.

The streamwise and normal velocity fluctuations u' and v' in the near-wake of the cylinder is mostly reduced by the influence of optimum acoustic control, which can be seen at the position $x/d = 1$ in Figs. 8(c) and (d). However, the velocity fluctuations near the separating shear-layers have increased, reflecting the appearance of a large velocity gradient, as seen in Fig. 8(a). It can be observed that the normal velocity fluctuation v' is more strongly suppressed by

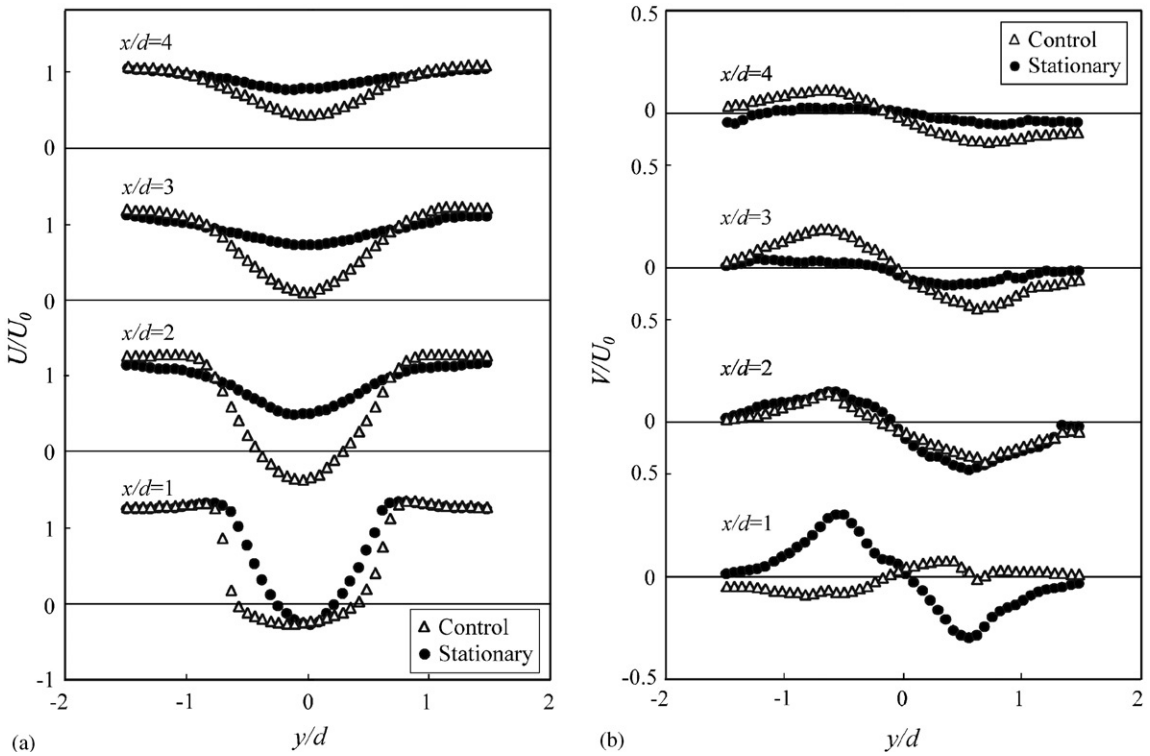

Fig. 8. Cross-sectional distributions of mean and fluctuating velocities: (a) mean velocity U; (b) mean velocity V; (c) velocity fluctuation u'; (d) velocity fluctuation v'; and (e) Reynolds stress $\overline{uv}$.

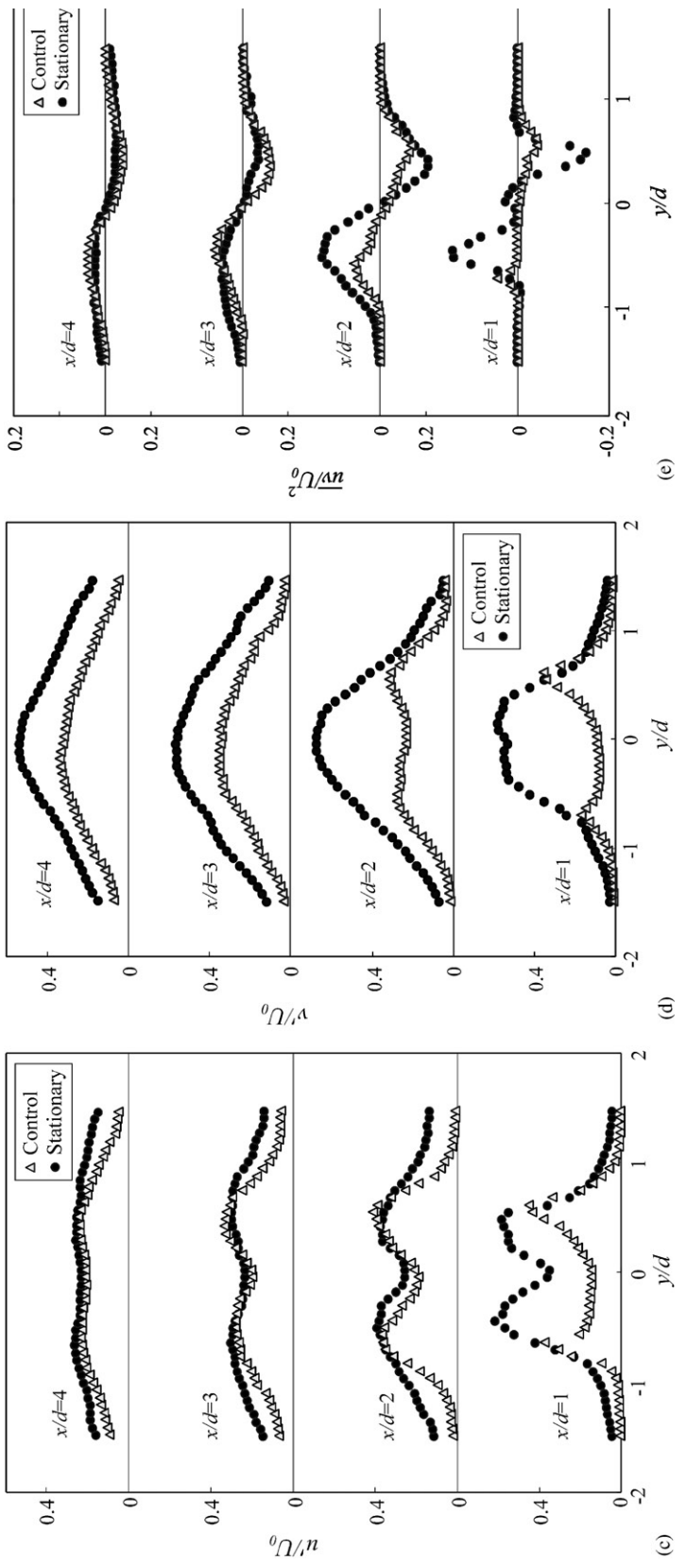

Fig. 8 (*continued*).

the control, so that the distribution of v' becomes even smaller than u' under the optimum acoustic control. It is to be noted that the reduction of the velocity fluctuations u', v' is caused by the presence of a small velocity gradient of U behind the cylinder, which can be seen in Fig. 8(a). The suppression effect of acoustic control on the velocity fluctuations u', v' is also seen in the distributions at $x/d = 2$, but their magnitudes are increased in comparison with those for $x/d = 1$, which reflects the change in velocity profiles U behind the cylinder with and without control. The influence of acoustic control is weakened as the streamwise distance increases to $x/d = 3$ and 4 and the velocity fluctuation u' and v' comes closer to those without control, but the influence is still observable even at the downstream station $x/d = 4$.

The observation of the Reynolds stress distribution $\overline{uv}$ is given in Fig. 8(e). The results under the optimum acoustic control show that the Reynolds stress behind the cylinder ($x/d = 1$) is very small, except for the region of separating shear-layers, which suggests that the generation of turbulent kinetic energy is very small in the near-wake of the cylinder. The smaller Reynolds stress in the near-wake region is attributed to the smaller gradient in the mean-velocity distribution behind the cylinder, which can be seen in Fig. 8(a). On the other hand, the Reynolds stress in the case without control is produced inside of the cylinder wake ($x/d = 1$) and its magnitude is much larger than the controlled case. It is to be noted that the large magnitude of the Reynolds stress in the uncontrolled case matches with the point of large velocity gradient in Fig. 8(a). With an increase in streamwise distance to $x/d = 2$, the magnitude of the Reynolds stress increases gradually and the peak of the Reynolds stress shifts inward under optimum acoustic control. However, the magnitude of the Reynolds stress of the uncontrolled case increases greatly at $x/d = 2$ and it spreads outward with an increase in downstream distance x/d. Although the magnitude of the Reynolds stress under optimum acoustic control comes closer to the uncontrolled case further downstream ($x/d = 3$, 4), the shape of the profile reflects the influence of the upstream flow history, so that the Reynolds stress profiles show different features with and without control at $x/d = 4$. Nevertheless, it can be considered that the variations of mean velocities and the corresponding suppression of velocity fluctuations and Reynolds stress in the cylinder wake support the observed drag reduction of the circular cylinder under optimum acoustic control.

4. Conclusions

The possible drag reduction of a circular cylinder in a uniform flow was studied by using an acoustic excitation technique, which was supplied internally, through a slit, to the flow over the cylinder. It was found from the experiment at Reynolds number 9000 that the drag of the circular cylinder is reduced at certain combinations of control parameters, such as the slit angle, the forcing Strouhal number and the excitation amplitude, which leads to a drag reduction of 30%. This condition was obtained when the acoustic excitation was given just behind the separation point with the frequency near the unstable frequency of the separating shear-layer. With larger amplitude of the acoustic excitation, the drag reduction is strengthened; however, it is saturated at larger values of excitation amplitude.

The wake velocity profile behind the circular cylinder and the statistical flow properties are measured by particle image velocimetry, with and without control. The wake velocity profile is modified by the acoustic control to be elongated downstream, and the reverse flow region is widened in the near-wake region behind the circular cylinder. Corresponding to the change of the mean-velocity field, the velocity fluctuations and the Reynolds stress in the near-wake region are strongly weakened under the conditions of optimum acoustic control. These results support the finding of drag reduction of a circular cylinder by acoustic excitation observed in the present experiment. However, further research would be useful in turbulent flows at higher Reynolds numbers for application to engineering problems. The response of the boundary layer and the wake of a circular cylinder to the acoustic excitation at high Reynolds numbers may deviate from those for low Reynolds number flow.

Acknowledgements

The authors would like to thank to Mr. G. Itabashi, Mr. T. Takano and the staff of the machine shop of Niigata University for their help with the experiment.

References

Bearman, P.W., 1984. Vortex shedding from oscillating bluff bodies. Annual Review of Fluid Mechanics 16, 195–222.
Blevins, R.D., 1985. The effect of sound on vortex shedding from cylinders. Journal of Fluid Mechanics 161, 217–237.

Blevins, R.D., 1990. Flow-Induced Vibration, 2nd Edition. Van Nostrad Reinhold, New York, pp.43–103.

Ffowcs Williams, J.E., Zhao, B.C., 1989. The active control of vortex shedding. Journal of Fluids and Structures 3, 115–122.

Filler, J.R., Marston, P.L., Mih, W.C., 1991. Response of the shear layers separating from a circular cylinder to small-amplitude rotational oscillations. Journal of Fluid Mechanics 231, 481–499.

Fujisawa, N., Ikemoto, K., Nagaya, K., 1998. Vortex shedding resonance from a rotationally oscillating cylinder. Journal of Fluids and Structures 12, 1041–1053.

Fujisawa, N., Kawaji, Y., Ikemoto, K., 2001. Feedback control of vortex shedding from a circular cylinder by rotational oscillations. Journal of Fluids and Structures 15, 23–37.

Griffin, O.M., Hall, M.S., 1991. Review; vortex shedding lock-in and flow control in bluff body wakes. ASME Journal of Fluids Engineering 113, 526–537.

Hsiao, F.B., Shyu, J.Y., 1991. Influence of internal acoustic excitation upon flow passing a circular cylinder. Journal of Fluids and Structures 5, 427–442.

Huang, X.Y., 1996. Feedback control of vortex shedding from a circular cylinder. Experiments in Fluids 20, 218–224.

Roussopoulos, K., 1993. Feedback control of vortex shedding at low reynolds numbers. Journal of Fluid Mechanics 24, 267–296.

Sarpkaya, T., 1979. Vortex-induced oscillations, a selected review. Journal of Applied Mechanics 46, 241–258.

Szeppesy, S., Bearman, P.W., 1992. Aspect ratio and end plate effects on vortex shedding from a circular cylinder. Journal of Fluid Mechanics 234, 191–217.

Tokumaru, P.T., Dimotakis, P.E., 1991. Rotary oscillation control of a cylinder wake. Journal of Fluid Mechanics 224, 77–90.

Warui, H.M., Fujisawa, N., 1996. Feedback control of vortex shedding from a circular cylinder by cross-flow oscillations. Experiments in Fluids 21, 49–56.